Semiconductor Physics, Quantum Electronics & Optoelectronics, 2014. V. 17, N 2. P. 134-148.

PACS 88.40.jm, 88.40.jp

New formalism for self-consistent parameters optimization of highly efficient solar cells

A.V. Sachenko[1], V.P. Kostylyov[1], M.R. Kulish[1], I.O. Sokolovskyi[1], A.I. Shkrebtii[2]
[1]V. Lashkaryov Institute of Semiconductor Physics, NAS of Ukraine
41, prospect Nauky, 03028 Kyiv, Ukraine
[2]University of Ontario Institute of Technology, Oshawa, ON, Canada
E-mail: sach@isp.kiev.ua

Abstract. We analyzed self-consistently photoconversion efficiency of direct-gap A^3B^5 semiconductors based solar cells and optimized their main physical characteristics. Using gallium arsenide (GaAs) as an example and new efficient optimization formalism, we demonstrated that commonly accepted light re-emission and reabsorption in solar cells in technologically produced GaAs (in particular, with solid- or liquid-phase epitaxy) are not the main factors responsible for high photoconversion efficiency. As we proved instead, the doping level of the base material and its doping type as well as Shockley-Read-Hall and surface recombination velocities are much more important factors responsible for this photoconversion. We found that the maximum photoconversion efficiency (about 27% for AM1.5 conditions) in GaAs with typical parameters of recombination centers can be reached for *p*-type base doped at $2\cdot10^{17}$ cm^{-3}. The open-circuit voltage V_{OC} formation features are analyzed. The optimization provides a significant increase in V_{OC} and the limiting photoconversion efficiency close to 30%. The approach of this research allows to predict the expected solar cell (for both direct- and indirect-gap semiconductor) characteristics, if material parameters are known. The applied formalism allows to analyze and to optimize mass production of both tandem solar cell and one-junction SC parameters.

Keywords: solar cell, efficiency, radiative recombination, saturation currents, doping, capture cross-section.

Manuscript received 16.01.14; revised version received 02.04.14; accepted for publication 12.06.14; published online 30.06.14.

1. Introduction

In recent years, an approach to the modeling of the tandem solar cells (TSC) limit photoconversion efficiency that considers photon recycling (re-emission and reabsorption of photons) in structures with multiple absorption of light as the key point was developed (see, e.g., [1, 2]). A point of view that there is a strong correspondence between the internal quantum yield of luminescence q_{pl} and photoconversion efficiency η (for defined model of the light absorption in the structure) is presented in these researches. The photoconversion efficiency in GaAs was calculated in papers [1, 2] as a confirmation of this concept. This material is not chosen by chance. On the one hand, GaAs is the key semiconductor when creating TSC based on direct-gap semiconductors of A^3B^5 group. On the other hand, in double heterostructures AlGaAs-GaAs-AlGaAs the internal luminescence quantum yield is close to 100% under certain conditions, as it was shown experimentally [3]. Therefore, the influence of reabsorption and re-emission of light on the efficiency

© 2014, V. Lashkaryov Institute of Semiconductor Physics, National Academy of Sciences of Ukraine

of solar cells based on GaAs was announced as very significant [1, 2].

However, as will be shown below, idealized assumptions used in [1, 2] are not being implemented in practice, and the implementation of typical semiconductor solar cell parameters are unsuitable for calculating and optimizing the parameters of a solar cell. Let us consider these assumptions in more detail. The basic assumption is the neglect of nonradiative recombination channels. The internal quantum yield of luminescence close to 100% is assumed. In fact, this value of q_{pl} was obtained in the laser structure with a high excitation level (~10^{17}cm^{-3}) [3]. In standard operation SC conditions, excitation is several orders of magnitude smaller. It leads to a substantial decrease in the internal quantum efficiency of luminescence. To prove it, we obtained, solved and analyzed in details the equation for the q_{pl} magnitude that is valid for an arbitrary excitation level and takes into account basic mechanisms of recombination.

Next approximation [1, 2] is the assumption that the light absorption coefficient α in high-purity gallium arsenide (doping level of semiconductor $\le 10^{14}\,\text{cm}^{-3}$) can be used for calculation of the short-circuit current and open-circuit voltage. In fact, as shown in this paper, even if implemented currently longest in GaAs Shockley-Read-Hall lifetimes ($\sim 10^{-6}\,\text{s}$), to get high values of the open-circuit voltage, it is necessary to implement the doping level of semiconductor $\ge 10^{17}\,\text{cm}^{-3}$. Thus, as shown in [5], the light absorption coefficient of doped GaAs is substantially different from that of the high-clean GaAs. As a result, the short-circuit current in *p*-type semiconductor increases and in *n*-type semiconductor decreases. Calculation of short-circuit current expressions for the internal quantum efficiency q_{SC} for cases where the diffusion length L significantly exceeds the SC thickness d, while the surface recombination velocity S is zero, was made [1, 2]. In this paper, much more general expression for q_{SC} is used for plane-parallel structures. It is valid in particular for arbitrary ratio between L and d, for arbitrary S and for any value of the light reflectance on the back surface R_d varying from 0 to 1.

Ding et al. [4] applied a more general approach [1, 2]. Calculation of the GaAs photoconversion efficiency [4] takes into account recombination in the space charge region (SCR) in recombination current calculation as well as the reabsorption and re-emission of photons. The saturation current I_{0r} is introduced for the implementation of $I-V$ curve non-ideality factor equal to 2. However, calculation [4] did not take into account Shockley-Read-Hall recombination current in the neutral part of base region. And there is no connection between the saturation current I_{0r} in [4] and such physical parameters as Shockley-Read-Hall recombination time τ_{SR}, the doping level of semiconductor, the effective densities of states in the conduction and valence bands as well as the bandgap. The model [4] does not allow to calculate the I_{0r} value for particular semiconductor and regarded structure parameters. It denies SC optimization by the recombination current minimization.

The extended and modified GaAs SCs efficiency analysis in this paper uses some results of [5]. In particular, this research is correct for the case of an arbitrary injection level, i.e. for an arbitrary excess (generated by the light) concentration Δp of electron-hole pairs. The luminescence internal quantum yield for arbitrary Δp is analyzed regarding main recombination mechanisms. The SCR recombination velocity and current corrected equations are determined and used to calculate the open-circuit voltage. The radiative recombination coefficient A is calculated using Roosbroeck and Shockley equations [6]. This work introduces self-consistent analysis of factors influencing the photoconversion efficiency in more general assumptions than those in [1, 2, 4].

In our work, the equation for the open-circuit voltage is written regarding the neutral part of the base region and SCR recombination currents. Saturation currents take into account radiative and nonradiative recombination and other semiconductor parameters, so the specific value of this ratio can lead to both the increase and decrease in this current. It is shown that this dependence in some cases is essential for the SC photovoltage calculation.

It is shown that the main SC parameters could not be chosen arbitrarily, because they are interdependent. For example, determining the doping level, it is necessary to consider the change in the light absorption coefficient and radiative recombination coefficient. It was found that reabsorption and re-emission of light are not major factors for the GaAs SCs efficiency.

These results can be used to select optimal parameters for SCs produced using both gallium arsenide and other semiconductor materials of industrial technologies (including germanium and silicon solar cells) and to achieve a maximum photoconversion efficiency.

2. Basic relations and the analysis of the influence of various factors on the GaAs photoconversion efficiency

Let us analyze GaAs photoconversion efficiency regarding the doping level and conductivity type, ratio of the cross-sections for carriers captured by deep levels, radiative and nonradiative recombination probabilities ratios for the SCR and the neutral part of the base region.

2.1. Influence of doping level and conductivity type

Let us analyze the behavior of the light absorption coefficient α of GaAs as a function of photon energy E_{ph}, depending on the conductivity type and the doping

© 2014, V. Lashkaryov Institute of Semiconductor Physics, National Academy of Sciences of Ukraine

level of semiconductor. These dependences $\alpha(E_{ph})$ are shown in Fig. 1 [5]. Fig. 1 shows the increase of the fundamental absorption edge blurry with increasing the doping level in *p*-type GaAs (Urbach effect), i.e. absorption increase in the spectral range where the photon energy E_{ph} is less than the bandgap E_g ($E_{ph} < E_g$). At the same time, in *n*-type GaAs at typical for TSCs levels of doping, there is electron gas degeneracy and Burstein-Moss effect domination. As a result, the doping level increase shifts the absorbtion edge to the high-energy region. Thus, the short-circuit current for a given thickness *d* decreases.

Using the known $\alpha(E_{ph})$ dependence [5] and the formula [6]

$$A = \frac{(kT)^3}{\pi^2 c^2 \hbar^3 n_i^2} \int_0^\infty \frac{\varepsilon(u)\alpha(u) u^2 du}{e^u - 1}, \quad (1)$$

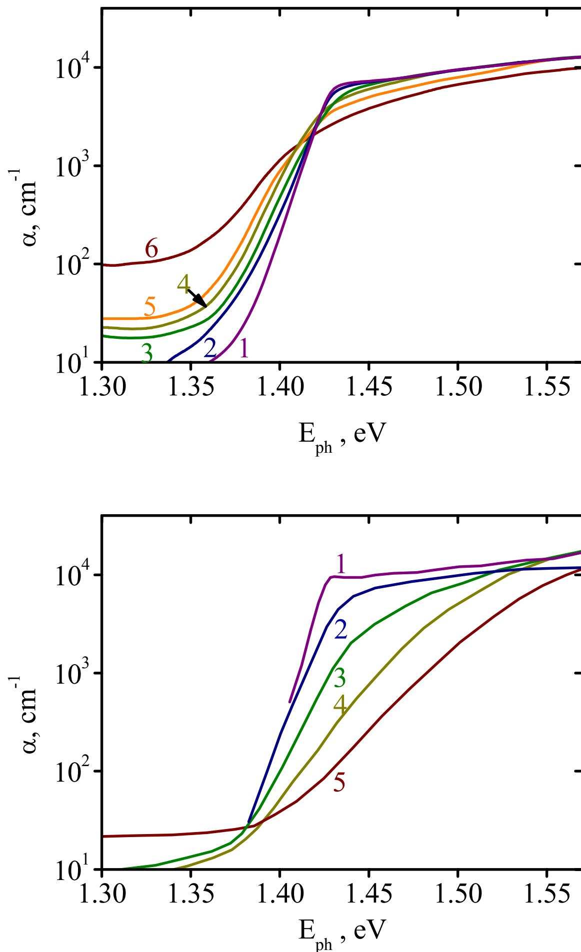

Fig. 1. Doping level influence on the absorption edge of *p*- (a) and *n*-type (b) GaAs [5]. *p*-type doping level, cm^{-3}: $1.6\cdot10^{16}$ (*1*), $2.2\cdot10^{17}$ (*2*), $4.9\cdot10^{17}$ (*3*), $1.2\cdot10^{18}$ (*4*), $2.4\cdot10^{18}$ (*5*), $1.6\cdot10^{19}$ (*6*); *n*-type doping level, cm^{-3}: $5\cdot10^{13}$ (*1*), $5.9\cdot10^{17}$ (*2*), $2\cdot10^{18}$ (*3*), $3.3\cdot10^{18}$ (*4*), $6.7\cdot10^{18}$ (*5*).

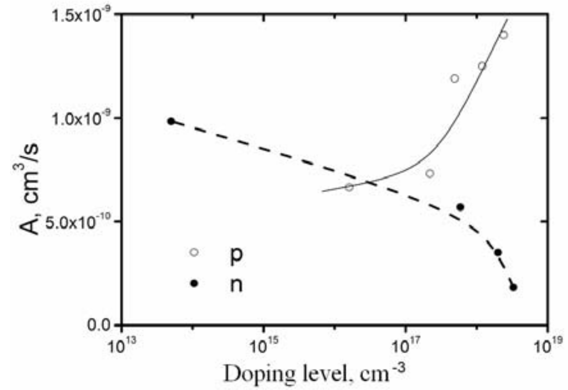

Fig. 2. The radiative recombination coefficient A versus the doping level in *n*- and *p*-type GaAs.

we can calculate the radiative recombination coefficient A. Here, c is the speed of light, $\hbar$ – Planck's constant, n_i – intrinsic concentration of semiconductor, $\varepsilon(u)$ – dielectric permittivity of semiconductor, taking into account the dispersion of the photon energy, $u = E_{ph}/kT$ – dimensionless photon energy.

The calculated values of A are shown in Fig. 2. The figure shows that in *p*-type semiconductors with the increasing doping level, the value A increases from $7\cdot10^{-10}\,\text{cm}^3/\text{s}$ for $p_0 = 10^{17}\,\text{cm}^{-3}$ up to $1.5\cdot10^{-9}\,\text{cm}^3/\text{s}$ for $p_0 = 2\cdot10^{18}\,\text{cm}^{-3}$. At the same time, in *n*-type semiconductors with the increasing doping level, the value A decreases from $10^{-9}\,\text{cm}^3/\text{s}$ for $n_0 = 10^{14}\,\text{cm}^{-3}$ down to $9\cdot10^{-11}\,\text{cm}^3/\text{s}$ for $n_0 = 2\cdot10^{18}\,\text{cm}^{-3}$.

The influence of the doping level on the value of bulk lifetime in GaAs [8-10] is shown in Fig. 3. In this case,

$$\tau_b = \left(\frac{1}{\tau_{SR}} + \frac{1}{\tau_r}\right)^{-1}, \quad (2)$$

where τ_{SR} is the Shockley-Read-Hall lifetime, $\tau_r = (A(N_d)N_d)^{-1}$ – radiative lifetime and N_d – doping level of the base. Fig. 3 shows that the bulk lifetime in *p*-type GaAs is lower than that in *n*-type. Data of Fig. 3 correlate with the data on the lifetimes for *n*- and *p*-type GaAs [9].

The contributions of τ_r and τ_{SR} can be separated using the known values of $A(N_d)$ and the relation (2). Using this way, the values of τ_{SR} for *n*- and p-type GaAs with different doping levels can be achieved. The typical τ_{SR} value is equal to $2\cdot10^{-8}\,\text{s}$ for *n*-type GaAs in the range of doping levels from $1\cdot10^{16}\,\text{cm}^{-3}$ up to $5\cdot10^{18}\,\text{cm}^{-3}$. For the doping level n_0 of $10^{16}\,\text{cm}^{-3}$, the

© 2014, V. Lashkaryov Institute of Semiconductor Physics, National Academy of Sciences of Ukraine

radiative lifetime τ_r is equal to 10^{-7} s, while for $n_0 = 2\cdot10^{18}\,\text{cm}^{-3}$ – $\tau_r = 2.5\cdot10^{-8}$ s. In the first case, τ_{SR} is less than τ_r, while in the second case the times τ_{SR} and τ_r are of the same order, i.e. radiative recombination does not dominate. For this case, photon recycling will be weakened even in highly reflective structures. Moreover, regarding to the photon recycling [4], the value of radiative recombination coefficient decreases. In this case, an effective radiative recombination coefficient $A_{eff} = A(1-\gamma_r)$ (here γ_r is the photon recycling factor) should be used in the open-circuit voltage V_{OC} calculation. This effect leads to the increase in the radiative lifetime and to the raise of nonradiative recombination contribution.

Typical τ_{SR} values in *p*-type semiconductors at low excitation levels ($\Delta p << p_0$) are about $5\cdot10^{-9}$ s [8, 9]. At sufficiently high levels of excitation, τ_{SR} is about $2.5\cdot10^{-7}$ s. Simple calculation allows using these values to determine the ratio of capture cross-sections for electrons and holes by recombination level, which in this case is equal to fifty.

Thus, as it follows from the analysis of known data about Shockley-Read-Hall lifetimes τ_{SR}, for typical τ_{SR} values in *n*- and *p*-type GaAs, *n*-type GaAs with higher τ_{SR} suites as the base material better. This doping type is also proposed in the Kayes patent [10].

2.2. Internal quantum efficiency of the short-circuit current

A more general expression for the quantum yield of the short-circuit current $q_{sc}(E_{ph})$ [11] can be written as

$$q_{SC} = q_{sp} + q_{sn}, \tag{3}$$

$$q_{sp} = \frac{\alpha L_p}{(\alpha L_p)^2 - 1}\cdot\frac{\alpha L_p + S_0\frac{\tau_p}{L_p}\left(1-e^{-\alpha d_p}\right)\cosh\left(\frac{d_p}{L_p}\right) - e^{-\alpha d_p}\sinh\left(\frac{d_p}{L_p}\right) - \alpha L_p e^{-\alpha d_p}}{S_0\frac{\tau_p}{L_p}\sinh\left(\frac{d_p}{L_p}\right) + \cosh\left(\frac{d_p}{L_p}\right)}, \tag{4}$$

$$q_{sn} = \frac{\alpha L e^{-\alpha d_p}}{1-(\alpha L)^2}\cdot\left\{\frac{\left[S_d\cosh\left(\frac{d}{L}\right) + \frac{D}{L}\sinh\left(\frac{d}{L}\right)\right]\left(1+R_d e^{-2\alpha d}\right) + \left(\alpha D(1-R_d) - S_d(1+R_d)\right)e^{-\alpha d} -}{S_d\sinh\left(\frac{d}{L}\right) + \frac{D}{L}\cosh\left(\frac{d}{L}\right)}\right.$$
$$\left.\frac{-\alpha L S_d\left[\sinh\left(\frac{d}{L}\right) + \frac{D}{L}\cosh\left(\frac{d}{L}\right)\right]\left(1-R_d e^{-2\alpha d}\right)}{S_d\sinh\left(\frac{d}{L}\right) + \frac{D}{L}\cosh\left(\frac{d}{L}\right)}\right\}. \tag{5}$$

Here, α is the light absorption coefficient, L_p – diffusion length in the emitter, d_p – thickness of the emitter, τ_p – bulk lifetime in the emitter, R_d – light reflection coefficient of the back surface, $L = (D\tau_b)^{1/2}$ – diffusion length in the base, D – diffusion coefficient in the base, S_0 – effective surface recombination velocity at the surface of the emitter, S_d – effective surface recombination velocity at the back surface.

When the $L >> d$ criterion fulfils, and when S_0 and S_d are small (compared to the recombination rate in the base volume), the expression for $q_S(E_g, E_{ph})$ reduces to $1-\exp(-\alpha d)$ expression for $R_d \to 0$ (poorly reflecting structures of the type A (Fig. 4)), and to expression $1-\exp(-2\alpha d)$ for $R_d \to 1$ (highly reflective structures of the type B (Fig. 4) [4]). However, for sufficiently low recombination times, when $L \le d$, as well as for large values of S_0 and S_d the short-circuit current quantum yield can be significantly reduced relative to the values above.

2.3. The open-circuit voltage

We obtained a more definite, than the commonly used, expression for the open-circuit voltage V_{OC} of solar cell with the $p-n$ junction. We suppose that in this expression the recombination current consists of two components: the neutral region recombination current and the base region SCR recombination current. Here we assume that Shockley-Read-Hall recombination goes through the discrete level close enough to the middle of the bandgap. Expressions for current recombination in SCR ([12] p. 104) can not be used directly for the illuminated SC. Furthermore, they are obtained in assumption of the equality of recombination center capture cross-sections of electrons and holes. We determine the contribution of SCR recombination in the open-circuit voltage V_{OC} and in the internal quantum yield of luminescence q_{pl} more correctly for a realistic case when cross-sections are not equal. At first, we

© 2014, V. Lashkaryov Institute of Semiconductor Physics, National Academy of Sciences of Ukraine

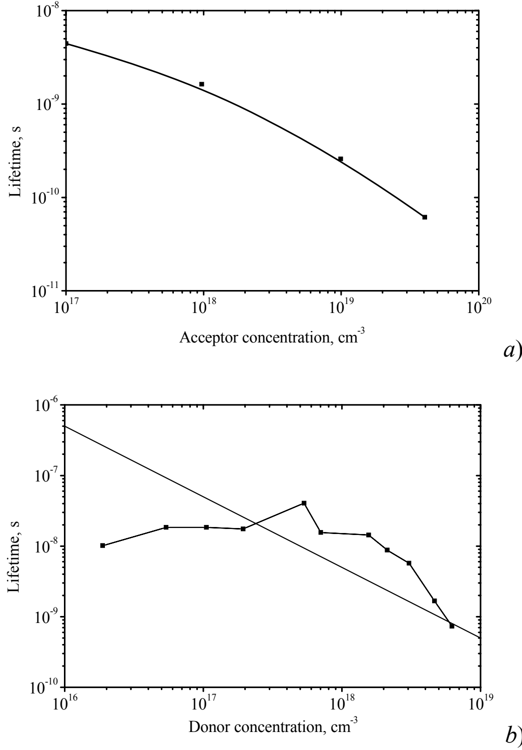

Fig. 3. Bulk lifetime in *p*- and *n*-type GaAs versus doping level [5]. Points are experimental values. Line in the figure for the *n*-type corresponds to the constant radiative recombination lifetime value.

Fig. 4. Schematic diagrams of two types of planar solar cell structures, labeled Structures A and B. Structure A is a semiconductor slab with an absorbing substrate, Structure B is a semiconductor slab with a reflecting substrate. Source: [4].

obtain the value of the recombination velocity in SCR V_{SC} for the illuminated SC, when recombination in SCR goes through a deep recombination level. We assume the concentration of recombination centers N_r, the capture cross-section of electrons σ_n and holes σ_p, energy placement is taken relative to the midgap. For *n*-type semiconductor under illumination, we can write

$$V_{SC}(\Delta p)=\frac{L_D}{\tau_{SR}}\int_{y_{pn}}^{0}\frac{n_0}{\left[(n_0e^{y}+n_ie^{\varepsilon_r})+b(p_0+\Delta p)e^{-y}+n_ie^{-\varepsilon_r}\right]\sqrt{-y+\left(e^{y}-1\right)+\frac{(p_0+\Delta p)}{n_0}e^{-y}}}\,dy\,. \quad (6)$$

Here, $L_D=\left(\varepsilon_0\varepsilon_S kT/2q^2n_0\right)^{1/2}$ is the Debye screening length, ε_0 – dielectric constant of vacuum, ε_S – relative permittivity of the semiconductor, k – Boltzmann constant, T – temperature, q – elementary charge, Δp – minority carriers excess concentration in the base, $\tau_{SR}=\left(C_pN_r\right)^{-1}$ – Shockley-Read-Hall lifetime, $C_p=V_T\sigma_p$, $C_n=V_T\sigma_n$, $b=\sigma_p/\sigma_n$ – carrier cross-sections ratio, V_T – carrier average thermal velocity, y_{pn} – the dimensionless potential at the $p-n$ junction interface, y – the actual dimensionless (normalized to kT/q) electrostatic potential,

$$n_i(T)=\sqrt{N_cN_v}\left(\frac{T}{300}\right)^{3/2}\exp\left(-\frac{E_g}{2kT}\right) \quad (7)$$

– intrinsic carriers concentration, N_c and N_v are effective densities of states in the conduction band and valence band for T = 300 K; E_g is the bandgap and $\varepsilon_r=E_r/kT$.

The same deep recombination center responsible for recombination in SCR and for Shockley-Read-Hall recombination in the neutral base region of SC is assumed in (6) for simplicity.

$V_{SC}(\Delta p)$ calculation shows that for $n_0\approx 10^7\,\text{cm}^{-3}$ and Δp ranged from $10^{12}\,\text{cm}^{-3}$ up to $10^{14}\,\text{cm}^{-3}$, corresponding to the SC operation conditions for different Shockley-Read-Hall recombination times, the recombination rate does not depend on the recombination energy position relative to the middle of bandgap E_r value up to ± 0.2 eV. Thus, when the E_r magnitude is less than 0.2 eV, the terms proportional to n_i in the denominator of expression (6) integrand can be neglected. It means that under these conditions the expression (6) for the SCR recombination velocity $V_{SC}(\Delta p)$, written for deep recombination centers, located in the middle of the gap, is correct for the high enough separation (within 0.2 eV) of the recombination level from the middle of the bandgap.

Using the expression (6) for E_r = 0 case, when sub-integral function has a maximum and $y_m=\ln(n_0/b(p_0+\Delta p))/2$ SCR recombination velocity V_{SC} can be written approximately as

$$V_{SC}=\frac{\kappa L_D}{\tau_{SR}}\frac{\left(\frac{n_0/b}{(p_0+\Delta p)}\right)^{1/2}}{\sqrt{\frac{1}{2}\ln\left(\frac{n_0/b}{(p_0+\Delta p)}\right)}}\,. \quad (8)$$

Here, κ is the constant of the order of 1. Calculations (1), (3) show κ increase from 1.9 to 2 with Δp increase from 10^{10} up to $10^{14}\,\text{cm}^{-3}$. In this case, the

© 2014, V. Lashkaryov Institute of Semiconductor Physics, National Academy of Sciences of Ukraine

calculation results by using the exact formula and approximate evaluation coincide with less than 5% error.

Fig. 5 shows the calculated $V_{SC}(E_g)$ dependences constructed using the formula (8). The parameter is the concentration Δp of minority holes in the base. One can see from the figure that starting from $10^{10}\,\text{cm}^{-3}$ V_{SC} is not dependent on E_g. The V_{SC} value decreases with the Δp increase.

When illumination makes $\Delta p >> p_0$, the relationship between V_{SC} and recombination saturation current density J_{rs} is described by the relation [13]

$$V_{SC} = \frac{J_{rs}}{q}\left(\frac{\Delta p}{p_0}\right)^{1/2} \Delta p^{-1}, \tag{9}$$

$$J_{rs} \approx \frac{q\,\kappa L_D b^{-1/2} n_i}{\tau_{SR}\sqrt{\frac{1}{2b}\ln\left(\frac{qn_0\left(d/\tau_b + S_S\right)}{J_g}\right)}}, \tag{10}$$

where $S_S = S_0 + S_d$.

The generation-recombination balance equation ignoring the SCR recombination

$$J_{SC} \approx q\left(\frac{d}{\tau_b} + S_S\right)\Delta p \tag{11}$$

was used in (10). The logarithm parameter in (10) is much greater than 1, so the first approximation can be used. Here, J_{SC} is the short-circuit photocurrent density. The equation (11) is correct, when the diffusion length L is greater than the base thickness d.

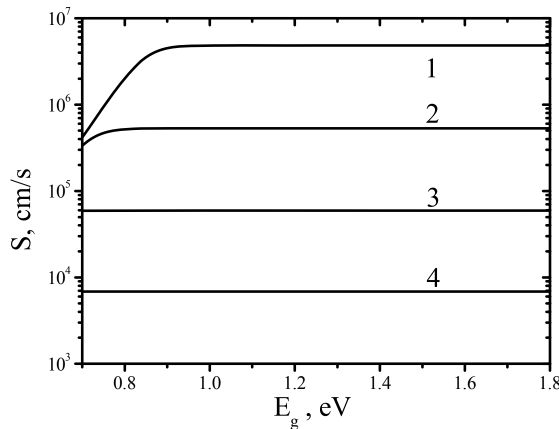

Fig. 5. Recombination velocity in SCR versus the bandgap for the following parameters: $\tau_{SR} = 10^{-7}$ s, $n_0 = 10^{17}\,\text{cm}^{-3}$, $T = 300$ K, $b = 10^{-2}$ s, Δp, cm^{-3}: *1* – 10^7; *2* – 10^9; *3* – 10^{11}; *4* – 10^{13}.

Taking into account SCR recombination, the open circuit voltage V_{OC} can be found via

$$J_g = q\left(\frac{d}{\tau_b} + S_S\right)\frac{n_i^2}{n_0}\left[\exp\left(\frac{qV_{OC}}{kT}\right) - 1\right] + q\frac{\kappa L_D b^{-1/2} n_i}{\tau_{SR}\sqrt{\frac{1}{2}\ln\left(\frac{1}{b}\frac{qn_0\left(d/\tau_b + S_S\right)}{J_g}\right)}}\left[\exp\left(\frac{qV_{OC}}{2kT}\right) - 1\right] \tag{12a}$$

when the second term is not much greater than the first one. If the second term is much more greater than the first one,

$$J_g = q\left(\frac{d}{\tau_b} + S_S\right)\frac{n_i^2}{n_0}\left[\exp\left(\frac{qV_{OC}}{kT}\right) - 1\right] + q\frac{\kappa L_D b^{-1/2} n_i}{\tau_{SR}\sqrt{\ln\left(\frac{\tau_{SR}}{q\kappa}\frac{J_g}{L_D n_i \exp\left(\frac{qV_{OC}}{2kT}\right)}\right)}}\left[\exp\left(\frac{qV_{OC}}{2kT}\right) - 1\right] \tag{12b}$$

should be used to find the open-circuit voltage V_{OC}.

2.4. The photoluminescence internal quantum yield

Let us write the expression for the photoluminescence internal quantum yield regarding radiative recombination, bulk Shockley-Read-Hall one, Auger, surface and SCR ones for arbitrary excitation level Δp. We consider *p*-type semiconductor in the calculation. We take into account both the Shockley-Read-Hall time and the surface recombination velocity dependence on the excitation value for $b \neq 1$. Let us consider such nonradiative recombination parameters dependences on the equilibrium majority carriers concentration p_0, minority carrier concentration n_0 and excitation level Δp as

$$\tau_{SR} = \tau_0\left(1 + b_b^{-1}\frac{n_0 + \Delta p}{p_0 + \Delta p}\right)^{-1},$$

$$S = S_0\left(1 + b_S^{-1}\frac{n_0 + \Delta p}{p_0 + \Delta p}\right)^{-1},$$

$$S_{SC} = S_{SC0}\left(\frac{b_b\, n_0}{\Delta p}\right)^{1/2}, \quad R_{\text{Auger}} = C\left(p_0 + \Delta p\right)^2. \tag{13}$$

Here, b_b and b_S are capture cross-sections relations for bulk and surface recombination levels, respectively, R_{Auger} is the Auger recombination rate, C – Auger recombination coefficient.

Thus, τ_{SR} and S dependences on Δp and other parameters of (13) are typical for the Shockley-Read-Hall recombination. S_{SC} dependence on Δp and other parameters is determined by (8).

Then in the case when $L > d$ (as required for efficient photoconversion), the expression for the

© 2014, V. Lashkaryov Institute of Semiconductor Physics, National Academy of Sciences of Ukraine

luminescence internal quantum efficiency can be written as

$$q_{pl} = \frac{d / \tau_r}{d\left(\tau_{SR}^{-1} + \tau_r^{-1}\right) + S + S_{SC} + R_{\text{Auger}}} . \quad (14)$$

Fig. 6 shows the calculated dependence of the luminescence internal quantum yield versus excitation level using the following parameters: $p_0 = 3 \cdot 10^{17}\,\text{cm}^{-3}$, $S_0 = 1{\cdot}10^2$ cm/s, $b_p = b_S = 0.02$ [9], $d = 1$ μm, $C = 7 \cdot 10^{-30}\,\text{cm}^6/\text{s}$ [3], S_{SC0} is calculated using (7). The following τ_0 values were used for 1-4 curves, respectively: $5{\cdot}10^{-9}$, $2 \cdot 10^{-8}$, $5{\cdot}10^{-8}$ and 10^{-6} s. Fig. 6 shows the luminescence internal quantum yield increase with the increase in τ_0 value. When $\tau_0 = 10^{-6}\,\text{s}$, q_{pl} value at its maximum is equal to 99.4%, which is very close to the value obtained in [3].

However, the Δp value in the SC under AM1.5 illumination is significantly lower. Δp is determined by the generation-recombination balance equation taking into account all recombination components:

$$J_{SC} / q = \left[d\left(\tau_{SR}^{-1} + \tau_r^{-1}\right) + S + S_{SC} + R_{\text{Auger}}\right] \Delta p . \quad (15)$$

The applied transcendent equations were solved numerically.

Fig. 7 shows Δp dependence on the Shockley-Read-Hall lifetime for A values of $5 \cdot 10^{-10}\,\text{cm}^3/\text{s}$ and $10^{-11}\,\text{cm}^3/\text{s}$. It can be seen that the curves for different A values coincide, when $\tau_{SR} \le 10^{-8}\,\text{s}$. The reason for this coincidence is in that $\Delta p \propto \tau_{SR}$ for this τ_{SR}, i.e. Δp is determined by the Shockley-Read-Hall recombination and does not depend on the radiative recombination. For these τ_{SR} values, the excitation level Δp increases linearly with τ_{SR} increase, and for τ_{SR} equal to $5 \cdot 10^{-9}\,\text{s}$ and $5 \cdot 10^{-8}\,\text{s}$ Δp equals to $2.9{\cdot}10^{11}$ and $2.9 \cdot 10^{12}\,\text{cm}^{-3}$, respectively. Correlating these values with q_{pl} dependences shown in Fig. 6, we find that for $b = 0.02$ and $\tau_{SR} = 5 \cdot 10^{-9}\,\text{s}$ the luminescence internal quantum yield q_{pl} in p-type semiconductor is about 7%, and for $\tau_{SR} = 2 \cdot 10^{-8}\,\text{s}$ $q_{pl} = 8\%$. For $b = 50$, the luminescence internal quantum yield q_{pl} rises up to 32% and 37%, respectively. And only for $\tau_{SR} = 10^{-6}\,\text{s}$ and $\Delta p \approx 1.3 \cdot 10^{14}\,\text{cm}^{-3}$, q_{pl} value is close to 93%. Thus, q_{pl} value is close to 100% only at laser excitation levels (obtained in [18]), when $\Delta p \ge 10^{17}\,\text{cm}^{-3}$. This situation does not correspond to the excitation levels of illuminated SC.

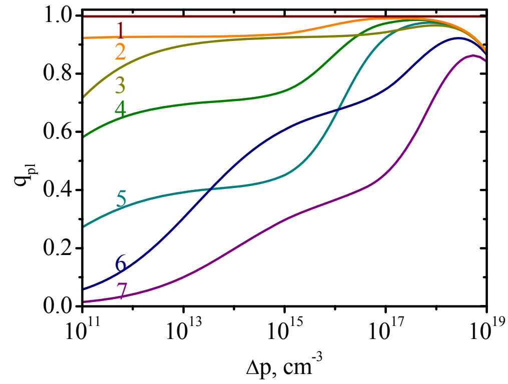

Fig. 6. Luminescence internal quantum yield versus the injection level. The used parameters: $p_0 = 3{\cdot}10^{17}$ cm^{-3}, $d = 10^{-4}$ cm, $A = 5{\cdot}10^{-10}$ cm^3/s, $S = 10^3$ cm/s, *1* – $\tau_{SR} = 10$ s, $b = 0.02$; *2* – $\tau_{SR} = 10^{-6}$ s, $b = 0.02$; *3* – $\tau_{SR} = 10^{-6}$ s, $b = 50$; *4* – $\tau_{SR} = 2{\cdot}10^{-8}$ s, $b = 0.02$; *5* – $\tau_{SR} = 2{\cdot}10^{-8}$ s, $b = 50$; *6* – $\tau_{SR} = 5{\cdot}10^{-9}$ s, $b = 0.02$; *7* – $\tau_{SR} = 5{\cdot}10^{-9}$ s, $b = 50$.

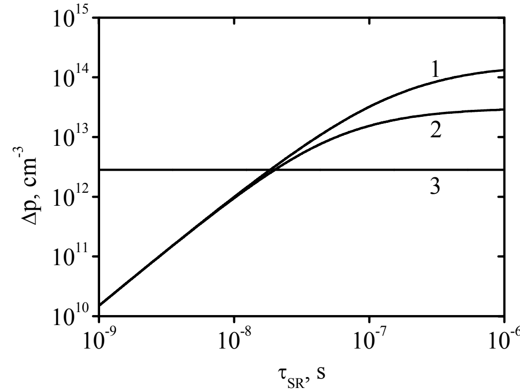

Fig. 7. Excitation level versus the Shockley-Read-Hall recombination lifetime. The used parameters: $p_0 = 10^{17}$ cm^{-3}, $d = 10^{-4}$ cm, $S = 10^3$ cm/s, $b = 0.02$, $J_{SC} = 30$ mA/cm^2, *1* – $A = 10^{-11}$ cm^3/s, *2* – $A = 5{\cdot}10^{-10}$ cm^3/s, *3* – $A = 5{\cdot}10^{-10}$ cm^3/s, $\tau_{SR} = 2{\cdot}10^{-8}$ s.

Note that in the estimates above, the absence of the surface recombination influence on the luminescence internal quantum yield was assumed. However, GaAs-AlGaAs system was used [3, 14] in the fabrication of structures with a high back surface reflectance, and the heterointerface recombination velocity lies within the range of 10^2–10^4 cm/s [15, 16]. For $\tau_b = \tau_r = 10^{-7}$ s, $d = 10^{-4}$ cm, $S_S = 10^3$ cm/s, the luminescence internal quantum yield q_{pl} is 33% (14). For $S_S > 10^3$ cm/s, for example, when $S_S = 10^4$ cm/s, we get even less q_{pl} value. In the latter case, even in the absence of bulk Shockley-Read-Hall recombination, the luminescence quantum yield is essentially reduced due to the GaAs-AlGaAs heterojunction recombination. Note that GaAs-AlGaAs system is the most matched and has the smallest lattice constants mismatch. All other heterostructures have greater lattice mismatch and therefore greater S_S values.

For *p-n* junction GaAs solar cells, the typical S_0 and S_d values are of the order of at least 10^5 cm/s [15]. The luminescence internal quantum yield q_{pl} for such SCs is significantly less than 1, so the effects of light re-

© 2014, V. Lashkaryov Institute of Semiconductor Physics, National Academy of Sciences of Ukraine

emission and reabsorption (photon recycling) can be neglected even for large τ_{SR} values.

2.5. The open-circuit voltage dependence on the semiconductor doping level

Using saturation currents [4] and considering the photon recycling, the maximum obtainable value of the open-circuit voltage in direct-gap semiconductors V_{OC} can be calculated (12). The radiative recombination saturation current density $J_{0r} = 7{\cdot}10^2$ A/cm^2 for B-type structures according to [4] was used to calculate the effective radiative recombination parameter A_{eff} from

$$J_{0r} = q A_{eff}\, d\, N_c N_v\,. \tag{16}$$

For $d = 2{\cdot}10^{-4}$ cm in highly reflective thick type B structures, the radiative recombination parameter A_{eff} is about $4{\cdot}10^{-12}$ cm^3/s, and for poorly reflecting type A structures (in which, according to [4] $J_{0r} \approx 1{\cdot}10^4$ A/cm^2), this parameter is about 10^{-10} cm^3/s. Substitution of the first value to the formula (12) by using the parameters of semiconductor with the bandgap 1.4 eV (as in [2]) neglecting nonradiative recombination gives the value 1.142 V for V_{OC}, which is only in fourth sign different from the V_{OC} value of 1.145 V [1, 2].

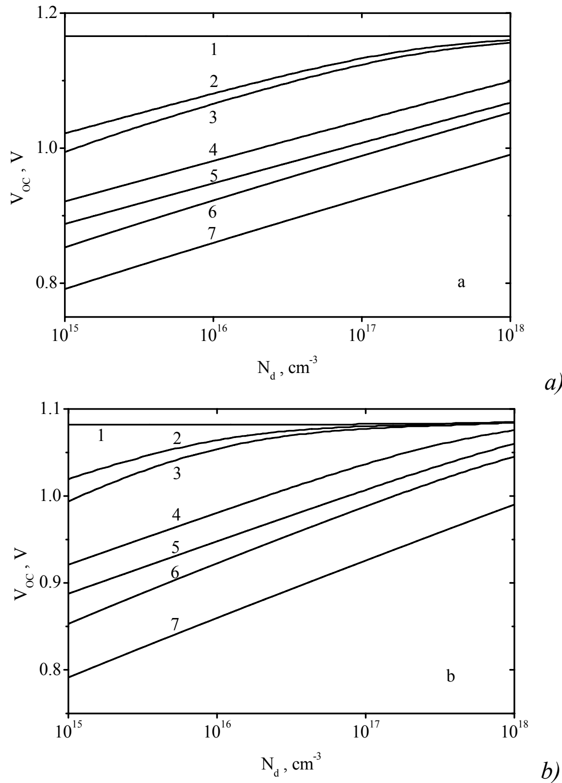

Fig. 8. Open-circuit voltage dependence on the doping level. The used parameters: $d = 10^{-4}$ cm, $\varepsilon_S = 12.8$, $S = 1$ cm/s, $T = 300$ K, $E_g = 1.42$ eV, $D = 10$ cm^2/s, $S = 1$ cm/s. Fig. 8a is calculated for $A_{eff} = 4{\cdot}10^{-12}$ cm^3/s, and Fig. 8b is calculated for $A_{eff} = 10^{-10}$ cm^3/s. The curves parameters for Fig. 8: *1* – τ_{SR} = 10 s, $b = 0.02$; *2* – $\tau_{SR} = 10^{-6}$ s, $b = 50$; *3* – $\tau_{SR} = 10^{-6}$ s, $b = 0.02$; *4* – $\tau_{SR} = 2{\cdot}10^{-8}$ s, $b = 50$; *5* – $\tau_{SR} = 2{\cdot}10^{-8}$ s, $b = 0.02$; *6* – $\tau_{SR} = 5{\cdot}10^{-9}$ s, $b = 50$; *7* – $\tau_{SR} = 5{\cdot}10^{-9}$ s, $b = 0.02$.

The calculated open-circuit voltage V_{OC} dependence for the type A and type B structures in the cases when $\tau_{SR} = 2\cdot 10^{-8}$s (curves 1 and 2), $\tau_{SR} = 10^{-6}$s (curves 3 and 4) and $\tau_{SR} = \infty$ (curves 5 and 6) on the doping level is plotted in Fig. 8. A_{eff} of 10^{-10}cm^3/s for the type A structures and A_{eff} of $4\cdot 10^{-12}$cm^3/s for the type B structures were used for Fig. 8 instead of A. The coincidence of $V_{OC}(n_0)$ dependences up to $n_0 = 10^{17}$ cm^{-3} for $\tau_{SR} = 2\cdot 10^{-8}$s with the calculated A_{eff} values means that in this doping levels area $V_{OC}(n_0)$ values are determined by nonradiative processes and are independent from the photon recycling. This dependence appears for $n_0 > 10^{17}$ cm^{-3}, but the $V_{OC}(n_0)$ value continues to grow fast enough with the n_0 increase.

The $V_{OC}(n_0)$ values differ markedly among themselves for $\tau_{SR} = 10^{-6}$s starting with the doping levels n_0 of 10^{16}cm^{-3}, but V_{OC} value growth with n_0 increase continues. The figure shows that $V_{OC}(n_0)$ dependence is growing up to $n_0 = 10^{18}$cm^{-3} except of the type A structures with $\tau_{SR} = 10^{-6}$s. The $V_{OC}(n_0)$ dependence is stronger than the $V_{OC}(A_{eff})$ dependence of Fig. 9 up to currently maximum Shockley-Read-Hall lifetimes of 10^{-6}s. For example, the $V_{OC}(A_{eff})$ value growth for $\tau_{SR} = 2\cdot 10^{-8}$s is equal to 1.5%, while the $V_{OC}(n_0)$ value growth is of 6%. Even for $\tau_{SR} = 10^{-6}$s, the $V_{OC}(A_{eff})$ value growth is of 8%, and the $V_{OC}(n_0)$ value growth is of 11%, i.e. V_{OC} growth with n_0 prevails. It should be noted that nonradiative recombination dominates for $V_{SC} > d/\tau_r$, i.e. even for the cases when Shockley-Read-Hall lifetime is not less than the radiative lifetime ($\tau_{SR} \ge \tau_r$). For example, for $\tau_{SR} = \tau_r = 10^{-7}$s and $d = 1$ μm the V_{SC} value exceeds d/τ_r value by six times.

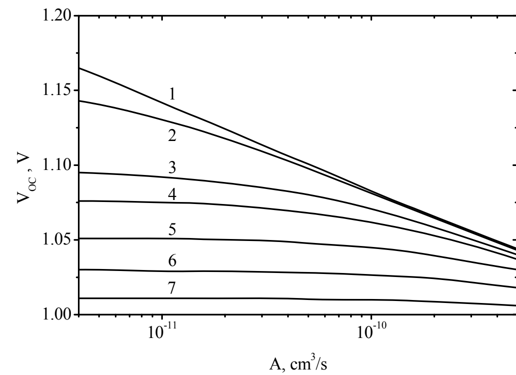

Fig. 9. Open-circuit voltage V_{OC} dependence on the radiative recombination coefficient A with account of nonradiative recombination. The used parameters: $n_0 = 2{\cdot}10^{17}$ cm^{-3}, $d = 2{\cdot}10^{-4}$ cm, $T = 300$ K, $E_g = 1.42$ eV, $D = 10$ cm^2/s, $S = 1$ cm/s, $\varepsilon_S = 12.8$, $b = 1$.

© 2014, V. Lashkaryov Institute of Semiconductor Physics, National Academy of Sciences of Ukraine

In conclusion, we note that the use of the J_{0r} = 10^4 A/cm^2 value for poorly reflecting structures and J_{0r} =7·10^2 A/cm^2 value for highly reflective structures leads to an overestimation of the photon recycling influence on the open-circuit voltage V_{OC} while radiative and nonradiative recombinations make comparable contributions. This is due to the use of 100% luminescence internal quantum yield in the light re-emission and reabsorption (photon recycling) [1, 2, 4].

If the luminescence internal quantum yield is reduced (for instance, from 100% down to 50%), only 1-2 successive reabsorption and re-emission acts will take place in highly reflective structures [1] instead of 30-40 acts. Thus, the J_{0r} value increases reducing the difference between A and A_{eff}. As a result re-emission and reabsorption processes influence will be decreased even earlier than the above calculations show. So, these formalisms are correct for V_{OC} calculation in the absence of nonradiative processes only. In intermediate cases of a comparable contribution of the radiative and nonradiative recombination to the open-circuit voltage V_{OC}, the V_{OC} values are less than values of Figs 8 and 9.

2.6. Influence of the capture cross-sections for electrons and holes on the open-circuit voltage

Since the recombination velocity in SCR V_{SC} and, therefore, the saturation current density depend on the ratio b for cross-sections of charge carriers captured by deep recombination levels, the open-circuit voltage V_{OC} will also depend on this ratio. According to (10) and (12), for $b > 1$ V_{SC} is decreased (so V_{OC} is increased) and for $b < 1$ V_{SC} is increased (so V_{OC} is decreased) in *n*-type semiconductors. The situation is reversed in *p*-type semiconductor, i.e. when $b > 1$ V_{OC} is decreased and when $b < 1$ V_{OC} is increased. Table 1 shows the *n*- and *p*-type gallium arsenide V_{OC} values, calculated for various b values. Table 1 shows that V_{OC} values can be significantly adjusted by the b value. Particularly, the V_{OC} value in *n*-type GaAs for $b = 0.02$ is smaller than the value in the *p*-type one even when the Shockley-Read-Hall lifetime τ_{SR} in the *n*-type exceeds τ_{SR} value in the *p*-type one. Thus, the b value should be considered in selection of the material for highly efficient solar cells.

Table 1. The influence of the ratio b of the cross-sections for electrons and holes captured by the deep recombination levels on the open-circuit voltage V_{OC} for different Shockley-Read-Hall lifetimes τ_{SR} .

b	τ_{SR} , s	V_{OC}, V
0.02	$5\cdot10^{-9}$	0.945
0.02	$8\cdot10^{-8}$	1.007
50	$5\cdot10^{-9}$	1.024
50	$2\cdot10^{-8}$	1.051
0.02	10^{-6}	1.080
50	10^{-6}	1.082

Table 2. The radiative recombination parameter A and short-circuit current density J_{SC} as functions of acceptor concentration N_a (*p*-type) and donor concentration N_d (*n*-type) in GaAs.

N_a, cm^{-3}	A, cm^3/s	J_{SC}, mA/cm^2
$1.6\cdot10^{16}$	$6.65\cdot10^{-10}$	31.663
$2.2\cdot10^{17}$	$7.32\cdot10^{-10}$	31.376
$4.9\cdot10^{17}$	$11.9\cdot10^{-10}$	30.642
$1.2\cdot10^{18}$	$12.5\cdot10^{-10}$	29.308
$2.4\cdot10^{18}$	$14.0\cdot10^{-10}$	27.271
$5\cdot10^{13}$	$9.84\cdot10^{-10}$	31.813
$5.9\cdot10^{17}$	$5.69\cdot10^{-10}$	27.400
$2\cdot10^{18}$	$3.51\cdot10^{-10}$	24.937
$3.3\cdot10^{18}$	$1.82\cdot10^{-10}$	24.815

2.7. Influence of the doping type and level on the short-circuit current

An analysis of the doping type and level influence on the short-circuit current magnitude is carried out on typical direct-gap semiconductor – gallium arsenide. Short-circuit current density under AM1.5 conditions in the case of full absorption of the incident light, neglecting SC illuminated surface shading by electrodes, is defined by the relationship:

$$J_{SC} = \left(1 - R_S\right)\left(1 - m\right)\int_{E_g}^{\infty} J_{AM1.5}\left(E_{ph}\right) q_{SC}(\alpha)\, dE_{ph} \,. \quad (17)$$

Here, R_S is the light reflection coefficient on the SC illuminated surface, m – illuminated surface shading by the contact grid factor, $J_{AM1.5}$ – spectral photocurrent density for AM1.5 illumination.

Since the gallium arsenide light absorption coefficient depends essentially on both doping level and conductivity polarity, this dependence should be taken into account in the short-circuit current J_{SC} calculation. The results of this calculation for gallium arsenide are shown in Table 2. It shows that J_{SC} value for *p*-type semiconductor increases with the doping level increase. This growth is associated with an increase in fundamental absorption edge blur with the doping level increase (see Fig. 1). At the same time, the J_{SC} value for *n*-type semiconductor decreases with the increase in doping level due to the conduction band filling by carriers (Burstein-Moss effect).

3. Direct-gap semiconductors photoconversion efficiency

Photoconversion efficiency calculation was fulfilled for GaAs SC as an example. The equation for *I*–*V* curve was written as

© 2014, V. Lashkaryov Institute of Semiconductor Physics, National Academy of Sciences of Ukraine

$$J(V) = J_{SC} - q\left(\frac{d}{\tau_b} + S_S\right)\frac{n_i^2}{n_0}\left[\exp\left(\frac{qV}{kT}\right) - 1\right] - \\ - q\frac{\kappa L_D b^{-1/2} n_i}{\tau_{SR}\sqrt{\frac{1}{2}\ln\left(\frac{qn_0(d/\tau_b + S_S)}{J_g b}\right)}}\left[\exp\left(\frac{qV}{2kT}\right) - 1\right]. \quad (18)$$

The photovoltage at maximum takeoff power V_m can be found from $d\{VJ(V)\}/dV = 0$ condition. The photocurrent density J_m for this case can be calculated by the substitution of V_m into (18). Finally, the photoconversion efficiency can be written as

$$\eta = \frac{J_m V_m}{P_S}, \quad (19)$$

where P_S is the illumination power density per unit area.

Fig. 10 shows the calculated using (19) GaAs photoconversion efficiency values versus the base material doping level for both conductivity polarities and the following Shockley-Read-Hall lifetimes τ_{SR}: $5 \cdot 10^{-9}$ s for *p*-type and $2 \cdot 10^{-8}$ s for the *n*-type. Zero R_S and m values were applied.

One can see from the figure that photoconversion efficiency η increases with the doping level growth for both *p*- and *n*-type. This increase is first of all due to an increase of V_{OC}. At higher doping levels, η decreases due to the interband Auger recombination predominance. Lower *n*-type SC η values in this region are associated with lower J_{SC} values. Maximum η values for both *p*- and *n*-type conductivity are realized at doping levels of about 10^{17} cm^{-3} and are close to the value of about 27% for typical τ_{SR} values. Thus, this doping level is optimal for the maximum efficiency η achievement in gallium arsenide.

Fig. 11 shows calculated η values versus the *b* value for *p*- and *n*-type gallium arsenide SCs. It can be seen that the maximum η values for *p*- and *n*-type gallium arsenide SCs are very similar, but the minimum values are much smaller for *n*-type. It is obvious that *n*-type Shockley-Read-Hall lifetime is less than the *p*-type lifetime. It leads to a significant V_m value decrease.

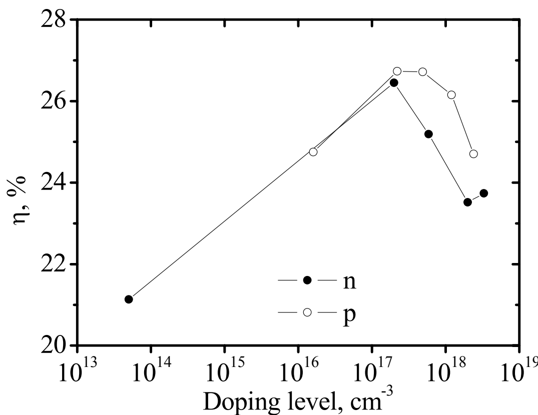

Fig. 10. Photoconversion efficiency dependence on the doping level.

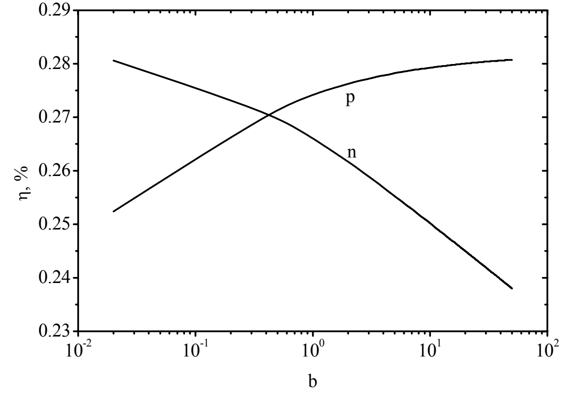

Fig. 11. Photoconversion efficiency versus the ratio *b* for the capture cross-sections of electrons and holes in GaAs. The used parameters: $n_0(p_0) = 2 \cdot 10^{17}$ cm^{-3}, $A = 5 \cdot 10^{-10}$ cm^3/s, $E_g = 1.42$ eV, $d = 10^{-4}$ cm, $\varepsilon_S = 12.8$, $S = 10^3$ cm/s; *p*-type: $J_{SC} = 31.6$ mA/cm^2, $\tau_{SR} = 5 \cdot 10^{-9}$ s, $D = 50$ cm^2/s; *n*-type: $J_{SC} = 30.9$ mA/cm^2, $\tau_{SR} = 2 \cdot 10^{-8}$ s, $D = 10$ cm^2/s.

Therefore, to achieve both high open-circuit voltage value and high short-circuit current density, i.e. to get the maximum photoconversion efficiency η, we must use *p*-type semiconductor as the base material. Note that the diffusion length of electrons in the *p*-type base material is much greater than the diffusion length of holes in the *n*-type base material. It is possible that the *p*-type GaAs disadvantage compared to the *n*-type is the lower Shockley-Read-Hall lifetime τ_{SR}. However, according to [7, 8], typical *p*-type lifetimes τ_{SR} are not so small compared to the *n*-type, so it is prematurely to do the final conclusions about the *n*-type.

We also note that, even for the maximum Shockley-Read-Hall lifetime of 10^{-6} s achieved, the photon recycling neglection leads to no more than 8% reduction in the case of highly reflective structures, and to no more than 3% reduction in the case of poorly reflecting structures. These differences are estimated to be not so great compared to, for example, the summarized influence of the ratio of the surface recombination velocity and cross-sections for electrons and holes captured by the recombination levels, especially with the doping level influence on the V_{OC} value. Therefore, the influence of these factors on the photoconversion efficiency must be considered in the first place.

4. Photoconversion efficiency analysis features for other semiconductors (the indirect and direct band)

The above relationships can be used to optimize the other direct-gap semiconductor solar cells (including A^3B^5 group) parameters. First of all, the article includes general relations allowing to fulfil a specified analysis. Second, a number of these semiconductor parameters are very close to the GaAs parameters. In particular, the electrons and holes effective masses that determine the mobility and diffusion coefficients in these semiconductors are very close to the GaAs ones.

© 2014, V. Lashkaryov Institute of Semiconductor Physics, National Academy of Sciences of Ukraine

Consequently, the densities of states in the conduction and the valence bands, as well as radiative recombination coefficients are close. The Shockley-Read-Hall lifetimes should be close as well. The single difference is the relation between the radiative and nonradiative processes in the semiconductor volume for these materials that changes in favor of the radiative processes dominance with the bandgap E_g decrease. So, the photon recycling growth for narrow-gap semiconductors is possible. However, the following two conditions have to be performed. First, this situation is possible only for small surface recombination velocity values. But the fulfilment of this condition is very difficult. The AlGaAs-GaAs systems, as mentioned, have interfaces of very high quality, with the lowest recombination velocities. Heterojunction interfaces of other semiconductors are not perfect, and the recombination velocities at the boundaries are much higher than those for the AlGaAs-GaAs system. This fact eliminates the role of the radiative processes.

Second, it is difficult to realize good light reflection conditions in the each cell of multi-junction SC, because it needs a certain relationship between the refractive indices of the neighbor cells. This condition limits the photon recycling again. Finally, the open-circuit voltage growth for the photon recycling is inessential for the actual Shockley-Read-Hall recombination times. Regarding to the faster open-circuit voltage decrease than the bandgap decrease with bandgap narrowing, the error due to the neglect of photon recycling in the total open-circuit voltage value for the typical τ_{SR} values will be small.

4.1. Indirect semiconductors (silicon)

The obtained relations can be used in a number of cases to optimize the indirect semiconductor (for example, silicon, germanium) solar cells parameters, in which the radiative recombination probability is low. Silicon and germanium are particularly used as a third element in some three-junction SCs. It is especially important for monocrystalline and multicrystalline silicon solar cells, as silicon solar modules and batteries are widely used. Moreover, monocrystalline and multicrystalline silicon SCs produce the prevalent part of electricity generated by direct solar energy conversion up to date.

Until recently, high-efficiency silicon solar cell parameters were modeled using the numerical solution of the drift and diffusion equations [9, 12]. There were also attempts [4, 17] to model silicon solar cells efficiency in the same approximations as gallium arsenide SCs, i.e. taking into account the photon recycling (re-emission and absorption of photons) in highly reflective structures or structures with multiple reflection (equal to the raise of the optical thickness). The photon recycling for silicon is assumed to be much lower than for gallium arsenide, where the luminescence internal quantum yield is assumed to be near 100% (as demonstrated for the high excitation case [3]). For example, the maximum photoluminescence external quantum yield of just 6.1% was obtained [18] at room temperature. To estimate the luminescence internal quantum yield q_{pl} for silicon, we use the equation (14) with the following interband Auger recombination parameter [11, 19]:

$$R_{\mathrm{Auger}} = C_p (p_0 + \Delta p)^2 + C_n (p_0 + \Delta p)\Delta p , \qquad (20)$$

where $C_p = 10^{-31}$ cm^6/s and $C_n = \left(2.8 \cdot 10^{-31} + \frac{2.5 \cdot 10^{-22}}{\Delta p^{0.5}} \right)$ cm^6/s. The second term in the expression for C_n includes the spatial correlation due to Coulomb interaction effect in the distribution of two electrons and one hole needed to act Auger recombination.

The $q_{pl}(\Delta p)$ calculation results for the case of silicon are shown in Fig. 12. The value of $6 \cdot 10^{-15}$ cm^3/s [20] was used as the radiative recombination parameter at $T = 300$ K. It can be seen from the figure (see curve 1) that the highest value of 99.3% is realized at $\Delta p = 10^{10}$ cm^{-3} and $p_0 = 10^{14}$ cm^{-3} for the case of interband Auger recombination, as the only nonradiative recombination channel is present. In the case of minimal recombination parameters (τ_{SR} = 38 ms, S = 0.25 cm/s) [21, 22] achieved in silicon, the largest q_{pl} value is 52.7% (curve 2). For the silicon solar cell parameters, providing the record efficiency equal to 25% [23], the highest q_{pl} value is 4% (curve 3). At $\Delta p \geq 10^{16}$ cm^{-3}, there is a strong q_{pl} drop associated with the increased nonradiative Auger recombination contribution. Since a typical Δp value for a silicon solar cell under illumination is greater than 10^{16} cm^{-3}, as it is shown by the calculation (15), q_{pl} value for this situation does not exceed 25%, as it is shown in Fig. 12. It means that the photon recycling can be neglected in the silicon solar cell parameters (including the maximum achievable one) simulation.

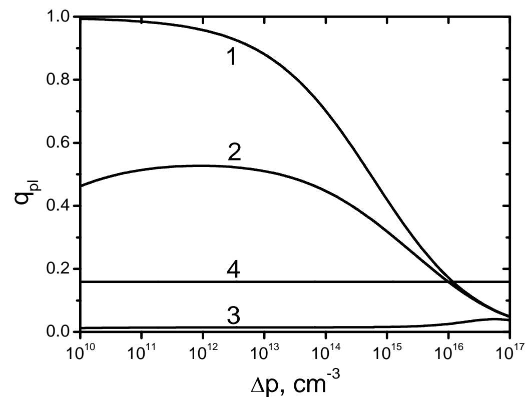

Fig. 12. Luminescence internal quantum yield dependence on the excitation level in silicon. The used parameters: $d = 200$ µm, $T = 298$ K; *1* – $p_0 = 3 \cdot 10^{16}$ cm^{-3}, $\tau_{SR} = 10^2$ s, $S = 10^{-3}$ cm/s; *2* – $p_0 = 8 \cdot 10^{16}$ cm^{-3}, $\tau_{SR} = 3.8 \cdot 10^{-2}$ s, $S = 10$ cm/s; *3* – $p_0 = 1 \cdot 10^{16}$ cm^{-3}, $\tau_{SR} = 10^{-3}$ s, $S = 60$ cm/s.

© 2014, V. Lashkaryov Institute of Semiconductor Physics, National Academy of Sciences of Ukraine

Note that the above formulae are not suitable for the silicon solar cell efficiency calculation in the case of over 20% efficiency. The matter is that these solar cells are manufactured from high quality monocrystalline silicon with the Shockley-Read-Hall lifetime not less than 1 ms. Therefore, the diffusion length L for such SCs can reach more than one millimeter, and this length substantially exceeds the base thickness d. The electron-hole pairs excess concentration in the open-circuit mode, as it has been said above, reaches values of the order of $10^{16}\,\text{cm}^{-3}$. If the base doping is less than this value, the open-circuit voltage V_{OC} in p-type semiconductor is determined by the following expression [11]

$$V_{OC} \cong \frac{kT}{q}\ln\left(\frac{\Delta p}{n_0}\right)+\frac{kT}{q}\ln\left(1+\frac{\Delta p}{p_0}\right). \qquad (21)$$

The greater $\Delta p / p_0$ ratio is in comparison to unity, the greater is the open-circuit voltage in a highly efficient silicon solar cell as compared to the case where $L < d$. This is associated not only with a higher Δp value, but also with the noticeable or even comparable to the illuminated surface voltage value contribution of the back surface to open-circuit voltage. Such a situation is never realized in direct-gap semiconductors, like to gallium arsenide, due to quite a short non-equilibrium charge carrier lifetime and $\Delta p << p_0$.

The 25% record photoconversion efficiency in silicon under AM1.5 conditions is set [23] especially for the case above where the formula (21) is correct. In addition to an almost complete incident light absorption by the SC implementation (that can be achieved through the use of geometric relief), the main problem is to minimize the surface recombination velocity values on the illuminated and back surfaces. The illuminated surface recombination velocity was minimized by thermal oxide with a low density of surface states growth and the back surface recombination velocity minimization was achieved by the isotype junction creation by Green [23]. There are recent researches solving this problem by $\alpha-\text{Si:H}-\text{Si}$ heterojunctions usage [24, 25]. In this case, dangling bonds passivation with hydrogen to minimize the surface recombination velocity S is necessary. The highest 24.7% efficiency of these solar cells was obtained in [25]. It is necessary to determine the Δp value from the equation (15) and substitute this Δp in (21) to find the V_{OC} value in this case.

Fig. 13 shows the V_{OC} dependence on the base doping level. The curve 1 corresponds to the limiting parameters, when the Shockley-Read-Hall recombination velocity and the surface recombination velocity are negligibly small as compared to the interband Auger recombination one. The curve 2 corresponds to the case of actual silicon parameters (τ_{SR} = 38 ms, S = 10 cm/s), and the curve 3 simulates the V_{OC} value for the silicon solar cell with a record efficiency of 25% [23]. All the curves have the maxima that lie at $p_0 \le 10^{17}\,\text{cm}^{-3}$ as can be seen from the figure. V_{OC} growth is associated with a relative decrease in the second term (21) contribution with the p_0 increase in the region of $p_0 < 10^{17}\,\text{cm}^{-3}$. V_{OC} decrease is associated with R_{Auger} growth for $p_0 \ge 10^{17}\,\text{cm}^{-3}$. The calculated using (21) open-circuit voltage value can exceed 0.740 V for the record SC parameters. Conventional silicon solar cells with $L < d$ can have such a V_{OC} value only under concentrated illumination.

The equation (21) is a quadratic equation as regards to Δp, and its solution has the following form:

$$\Delta p = -\frac{p_0}{2}+\sqrt{\frac{p_0^{\,2}}{4}+\exp\left(\frac{qV_{OC}}{kT}\right)}. \qquad (22)$$

Replacing V_{OC} in (22) by the applied forward bias V, we get the Δp to V relation. It allows to write current-voltage characteristic based on the expression (15)

$$J(V) = J_{SC} - J_{rec}(V). \qquad (23)$$

Further, we find V_m from the maximum takeoff power condition $d(VJ(V))/dV = 0$, and its substitution in (23) allows the J_m value determining. As a result, we obtain the silicon solar cell photoconversion efficiency under AM 1.5 illumination:

$$\eta = \frac{J_m V_m}{P_S}. \qquad (24)$$

Fig. 14 shows the photoconversion efficiency dependence on the Shockley-Read-Hall lifetime τ_{SR}. The basic parameters are the same as those in the previous figure. As one can see from the figure, for sufficiently large τ_{SR} values η reaches its maximum and saturates. Saturation comes earlier for the larger S values.

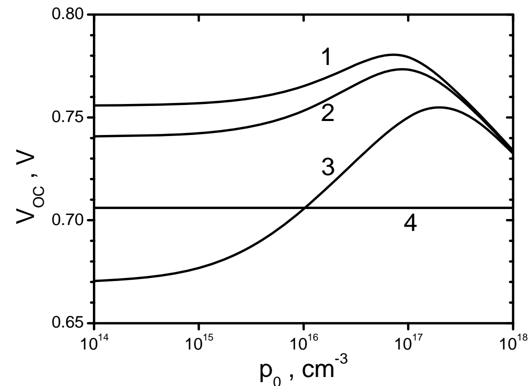

Fig. 13. Open-circuit voltage dependence on the doping level. The used parameters: d = 200 µm, T = 298 K. The same τ_{SR} and S values as for Fig. 12. The short-circuit current density J_{SC} was assumed as: *1* – 43.5 mA/cm^2, *2* – 42.7 mA/cm^2, *3* – 42.7 mA/cm^2.

© 2014, V. Lashkaryov Institute of Semiconductor Physics, National Academy of Sciences of Ukraine

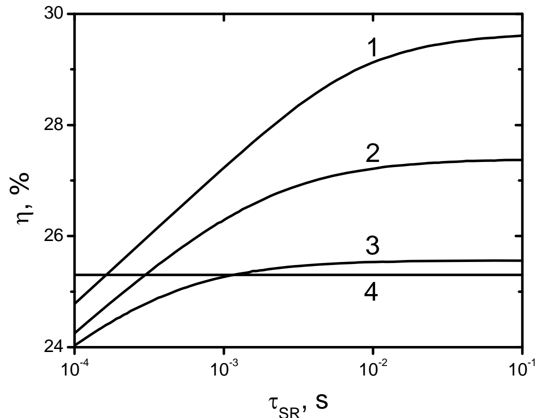

Fig. 14. Photoconversion efficiency η versus the lifetime τ_{SR}. The used parameters: d = 200 μm, T = 298 K. The same S values as for Fig. 13. The doping level was assumed to be 10^{16} cm^{-3}.

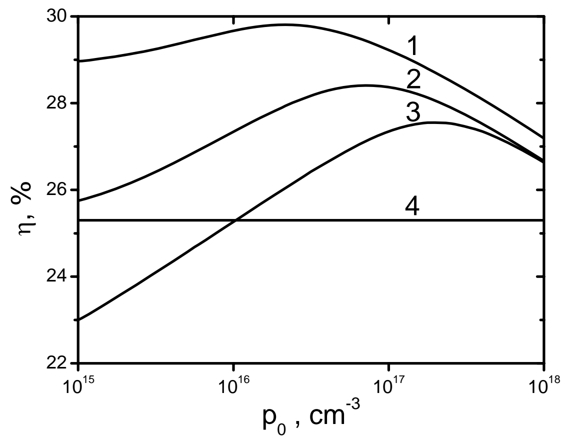

Fig. 15. Photoconversion efficiency η versus the doping level. The used parameters: d = 200 μm, T = 298 K. The same parameters as for Fig. 13.

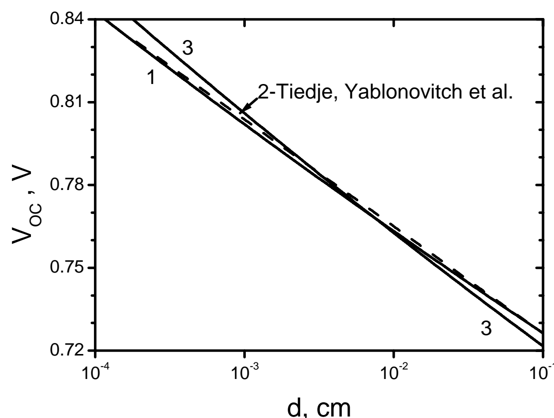

Fig. 16. Calculated open-circuit voltage versus the thickness of the limit silicon solar cell obtained in [17] (*1*), calculated using the parameters of [17] (*2*) and calculated using the parameters of our papers [19, 20] (*3*).

Table 3. Experimental and calculated values of the main silicon solar cell parameters for three different samples [23-25].

Number of cell	J_{SC}^{exp}, mA/cm^2	V_{OC}^{exp}, V	V_{OC}^{th}, V	η_{exp}, %	η_{th}, %
1	427	0.706	0.706	25	25.3
2	394	0.745	0.745	23.7	23.8
3	395	0.750	0.750	24.7	24.9

Fig. 15 shows the η dependence on the base doping level p_0, which is calculated with the same basic parameters. It can be seen that all three curves have maxima. The lower p_0 values in maxima are realized for smaller Shockley-Read-Hall recombination and surface recombination contributions in complete recombination. The maximum attainable η value for these parameters is 29.2%. If the solar cell thickness decreases from 200 to 50 μm, the limiting η value increases to 30.4%.

Next, let us to write theoretical equations for open-circuit voltage and photoconversion efficiency versus base doping level for 25%-effective record silicon solar cell [23], as well as for silicon solar cells with surface recombination, minimized by the $\alpha-\mathrm{Si:H}-\mathrm{Si}$ heterojunctions [24, 25] using the above formalism. First, the recombination parameters for V_{OC} of 706 mV obtained in [23] are calculated. They are determined from the curve 3 in Fig. 13 intersection with the experimental value 706 mV. Next, we substitute the parameters, for which this coincidence was obtained, and the experimental short-circuit current density value equal to 42.7 mA/cm^2, in the expression for η. As a result, η = 25.3% is achieved. The relevant parameters for the $\alpha-\mathrm{Si:H}-\mathrm{Si}$ heterojunction solar cells [24, 25] were calculated in the similar manner. The final results are presented in Table 3. It can be seen from the table that the calculated open-circuit voltage values coincide with the experimentally obtained in all the cases. The matching error between the calculated and the experimental η values is less than 1%. These results demonstrate the adequacy of the theoretical model proposed in this paper relative to the experimental results obtained in [23 – 25].

In conclusion, we compare the results obtained in this work with the results of the research [17]. In this paper, Fig. 8 shows the results of the open-circuit voltage calculation depending on the silicon solar cell thickness taking into account radiative recombination and interband Auger recombination. These dependences are calculated using expressions (21) and (15). First, let us correct the parameters to those of [17]. Thus, we assume that the intrinsic charge carriers concentration in silicon (for T = 300 K) equals to $1.45\cdot10^{10}\,\mathrm{cm}^{-3}$, and the radiative recombination coefficient equals to $2.5\cdot10^{-15}\,\mathrm{cm}^3/\mathrm{s}$ [17]. Let us also omit the

© 2014, V. Lashkaryov Institute of Semiconductor Physics, National Academy of Sciences of Ukraine

$2.5\cdot10^{-22}/\Delta p^{0.5}$ term in C_n that is absent in [17]. The comparison of the $V_{OC}(d)$ dependences calculated using the formulae (15) and (21) of our work (Fig. 16, curve 1) with those achieved in [17] (Fig. 8) (see Fig. 16 of this paper, curve 2) show a good agreement. This figure also shows the $V_{OC}(d)$ curves constructed using the formulae (15) and (21) of this paper and the parameters of silicon from [19, 20] (curve 3). There is a good coincidence of the curves (1) and (3), which are practically the same for the actual silicon solar cell thickness (close to 100 µm), although they are different for small and large SC thicknesses. A little higher $V_{OC}(d)$ values at small thickness values are associated with the use of lower hole and electron concentrations in silicon equal to $8.5\cdot10^{9}\,\text{cm}^{-3}$. Lower $V_{OC}(d)$ values at large thickness values are explained by the greater radiative recombination parameter at room temperature ($6\cdot10^{-15}\,\text{cm}^3/\text{s}$) and by taking into account the additional term in the relation for C_n.

The limiting silicon solar cells photoconversion efficiency in our work correlates with that obtained in [17], and is consistent with the conclusions of [26]. However, the photon recycling for calculating the silicon solar cells parameters (including the maximum possible and record) can be neglected, as shown by the results of our analysis, in contrast to [4, 17]. As a result, the calculation is greatly simplified and can be performed in the traditional approximations.

5. Conclusions

An approach to optimize SC based on direct- and indirect-gap semiconductors in order to obtain the maximal photoconversion efficiency has been proposed.

Analysis shows the secondary role of photon recycling even in highly reflective structures for commercial GaAs parameters, particularly typical Shockley-Read-Hall recombination lifetime τ_{SR} values. The open-circuit voltage V_{OC} enhancement by the doping level optimization has been shown to be much more critical for photoconversion efficiency growth. The optimal doping level of about $10^{17}\,\text{cm}^{-3}$ has been determined. The maximal photoconversion efficiency η_{max} for such condition is near 27%.

The doping level and polarity type influence on the GaAs absorption coefficient and photoconversion efficiency has been studied. It has been shown that the conduction band filling with electrons and the respective increase in the donor doping level (Burstein-Moss effect for *n*-type semiconductor) leads to a decrease in the short-circuit current. The fundamental band edge blur increase (Urbach shift) leads to an increase in the short-circuit current for *p*-type semiconductor.

The influence of the ratio *b* of the cross-sections for electrons and holes captured by the deep recombination levels on the open-circuit voltage and, consequently, the photoconversion efficiency has been demonstrated.

The developed formalism allows to analyze and to optimize SC parameters for other direct-gap semiconductors, particularly in A^3B^5 semiconductors.

The open-circuit voltage and photoconversion efficiency generation features for monocrystalline silicon solar cells with more than 1 ms Shockley-Read-Hall lifetime have been considered.

A formalism describing quantitatively the experimental results for high-efficiency silicon solar cells using various surface recombination velocity minimization techniques has been also proposed.

The approach of this research allows to predict the expected solar cell (for both direct- and indirect-gap semiconductors) characteristics, if material parameters are known.

References

1. O.D. Miller, E. Yablonovitch and S.R. Kurtz, Strong internal and external luminescence as solar cells approach the Shockley–Queisser limit // *IEEE J. Photovoltaics*, **2**(3), p. 303-311 (2012).
2. O. Miller *Photonic Design: From Fundamental Solar Cell Physics to Computational Inverse Design*, Doctoral dissertation. University of California, Berkeley, USA, 2012, 137 p.
3. I. Schnitzer, E. Yablonovitch, C. Caneau and T.J. Gmitter, Ultrahigh spontaneous emission quantum efficiency, 99.7% internally and 72% externally, from AIGaAs/GaAs/AIGaAs double heterostructures // *Appl. Phys. Lett.* **62**(2), p. 131-133 (1993).
4. D. Ding, S.R. Johnson, S.-Q. Yu, S.-N. Wu and Y.-H. Zhang, A semi-analytical model for semiconductor solar cells // *J. Appl. Phys*. **110**, 123104 (2011).
5. H.C. Casey, D.D. Sell, and K.W. Wecht, Concentration dependence of the absorption coefficient for n- and p-type GaAs between 1.3 and 1.6 eV // *J. Appl. Phys*. **46**(1), p. 250-257 (1975).
6. W. Van Roosbroeck, W. Shokley, Photon-radiative recombination of electrons and holes in germanium // *Phys. Rev.* **94**(6), p. 1558-1560 (1954).
7. G.B. Lush, H.F. MacMillan, B.M. Keyes, D.H. Levi, R.K. Ahrenkiel, M.R. Melloch and M.S. Lundstrom, A study of minority carrier lifetime versus doping concentration in n-type GaAs grown by metalorganic chemical vapor deposition // *J. Appl. Phys*. **72**(4), p. 1436-1442 (1992).
8. Hiroshi Ito, Tomofumi Furuta and Tadao Ishibashi, Minority electron lifetimes in heavily doped p-type GaAs grown by molecular beam epitaxy // *Appl. Phys. Lett.* **58**(25), p. 2936-2938 (1991).
9. A.L. Fahrenbruch and R.H. Bube. *Fundamentals of Solar Cells. Photovoltaic Solar Energy Conversion*. New York, 1983.
10. H. Nie, B.M. Kayes and I. Kizilyalli, Optoelectronic devices including heterojunction. *EP Patent 2,450,956.*

© 2014, V. Lashkaryov Institute of Semiconductor Physics, National Academy of Sciences of Ukraine

11. A.P. Gorban, A.V. Sachenko, V.P. Kostylyov and N.A. Prima, Effect of excitons on photoconversion efficiency in the p^+-n-n^+- and n^+-p-p^+-structures based on single-crystalline silicon // *Semiconductor Physics, Quantum Electronics and Optoelectronics*, **3**(3), p. 322-329 (2000).
12. S.M. Sze and Kwok K. Ng, *Physics of Semiconductor Devices*, 3rd Ed. John Wiley and Sons, 2007.
13. A.P. Gorban, V.P. Kostylyov, A.V. Sachenko, O.A. Serba, I.O. Sokolovskyi, V.V. Chernenko, Effect of floating *p-n* junctions on the efficiency of silicon back side contact solar cells // *Ukr. J. Phys.* **55**(7), p. 783-790 (2010).
14. B.M. Kayes, H. Nie, R. Twist, S.G. Spruytte, F. Reinhardt, I.C. Kizilyalli, G.S. Higashi, 27.6% conversion efficiency, a new record for single-junction solar cells under 1 sun illumination // *Photovoltaic Specialists Conference (PVSC), 2011 37th IEEE* , p. 000004-000008, June 19-24, 2011.
15. P.A. Folkes, B. Connelly and F. Towner, Minority carrier lifetime and interfacial recombination velocity in GaAs/AlGaAs double heterostructures // *ARL-TR-6186 Report.*
16. R.I. Jioev, K.V. Kavokin, Optical measurement of diffusion length and electron surface recombination velocity in the *p*-GaAs layers // *Fizika i tekhnika poluprovodnikov*, **33**(10), p. 2928-2931 (1991), in Russian.
17. T. Tiedje, E. Yablonovitch, G.D. Cody and B.J. Brooks, Limiting efficiency of silicon solar cells // *IEEE Trans. on Electron Devices*, **31**(5), p. 711-716 (1984).
18. T. Trupke, J. Zhao, A. Wang, R. Corkish, M.A. Green, Very efficient light emission from bulk crystalline silicon // *Appl. Phys. Lett.* **82**, p. 2996-2998 (2003).
19. A.V. Sachenko, A.P. Gorban, V.P. Kostylev, I.O. Sokolovskii, Quadratic recombination in silicon and its influence on the bulk lifetime // *Semiconductors*, **41**(3), p. 281-284 (2007).
20. A.V. Sachenko, A.P. Gorban, V.P. Kostylyov, I.O. Sokolovsky, The radiative recombination coefficient and the internal quantum yield of electroluminescence in silicon // *Semiconductors*, **40**(8), p. 884-889 (2006).
21. E. Yablonovitch and T. Gmitter, Auger recombination in silicon at low carrier densities // *Appl. Phys. Lett.* **49**(10), p. 587-589 (1986).
22. E. Yablonovitch, D.L. Allara, C.C. Chang, T. Gmitter and T.B. Bright, Unusually low surface-recombination velocity on silicon and germanium surfaces // *Phys. Rev. Lett.* **57**(2), p. 249-252 (1986).
23. M.A. Green, The path to 25% silicon solar cell efficiency: History of silicon cell evolution // *Progr. Photovolt.: Res. Appl.* **17**(3), p. 183-189 (2009).
24. T. Sawada, N. Terada, Sadaji Tsuge, Baba Toshiaki, T. Takahama, Kenichiro Wakisaka, Shinya Tsuda, Shoichi Nakano, High-efficiency a-Si/c-Si heterojunction solar cell // *1994 IEEE First World Conference on Photovoltaic Energy Conversion,* Conference Record of the Twenty Fourth IEEE Photovoltaic Specialists Conference, p.1219-1226 (1994).
25. A. Yano, S. Tohoda, K. Matsuyama, Y. Nakamura, T. Nishiwaki, K. Fujita, M. Taguchi, E. Maruyama, 24.7% record efficiency HIT® solar cell on thin silicon wafer // *28th European Photovoltaic Solar Energy Conference and Exhibition,* September 30–October 4, 2013, Paris, France, p. 748-751.
26. R.M. Swanson, Approaching the 29% limit efficiency of silicon solar cells // *20 European Photovoltaic Conference*, June 6-10, 2005, Barcelona, Spain, p. 584-589.

© 2014, V. Lashkaryov Institute of Semiconductor Physics, National Academy of Sciences of Ukraine